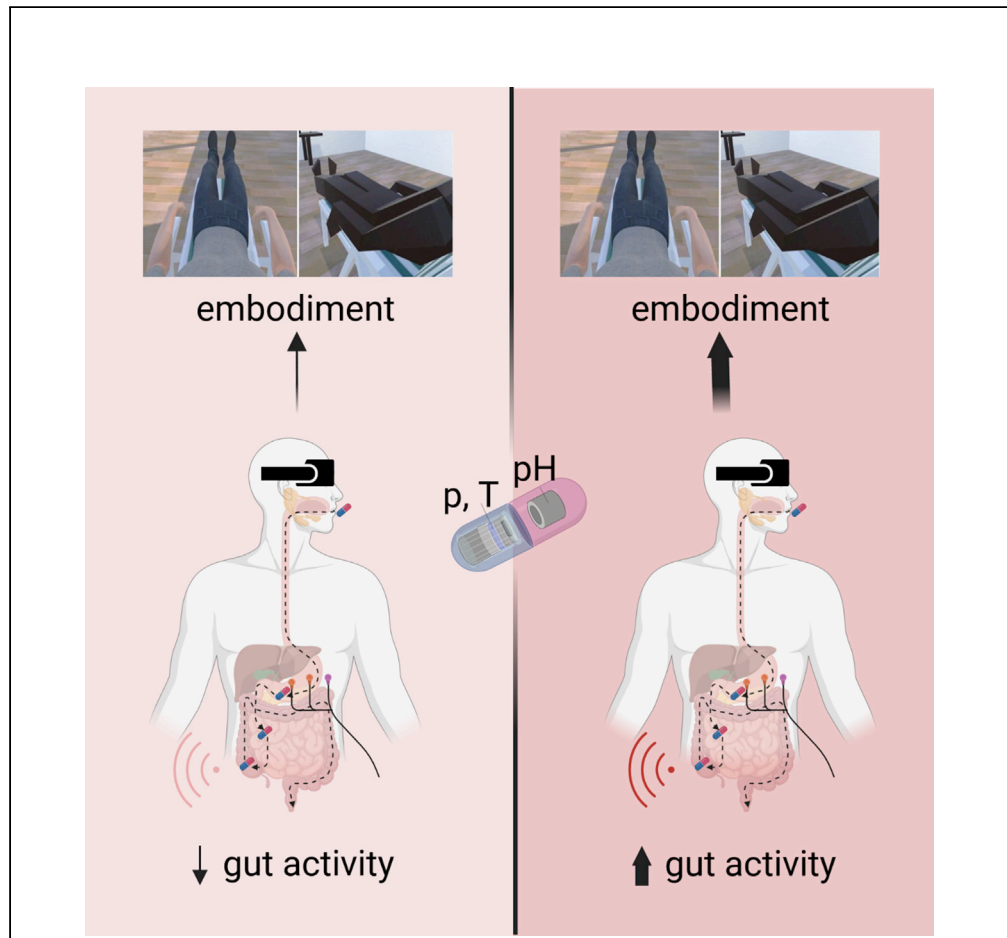**Article**

Gut markers of bodily self-consciousness in men

Alessandro Monti,
Giuseppina
Porciello, Maria
Serena Panasiti,
Salvatore M.
Aglioti

alessandro.monti@uniroma1.it
(A.M.)
salvatoremaria.aglioti@
uniroma1.it (S.M.A.)

Highlights

We studied the
gastrointestinal (GI)
underpinnings of bodily
self-consciousness

An ingestible pill tracked
how GI parameters
change during a bodily
illusion

GI activity was generally
correlated with higher
embodiment and lower
disembodiment

Gut plays a significant role
in how our self embodies
entities such as avatars

Article

Gut markers of bodily self-consciousness in men

Alessandro Monti,[1,4,*] Giuseppina Porciello,[2,3] Maria Serena Panasiti,[2,3] and Salvatore M. Aglioti[1,2,*]

SUMMARY

Bodily self-consciousness, the state of mind that allows humans to be aware of their own body, forms the backdrop for almost every human experience, yet its underpinnings remain elusive. Here we combine an ingestible, minimally invasive capsule with surface electrogastrography to probe if gut physiology correlates with bodily self-consciousness in a sample of healthy men during a virtual bodily illusion. We discover that specific patterns of stomach and bowel activity (temperature, pressure, and pH) covary with specific facets of bodily self-consciousness (feelings of body location, agency, and disembodiment). These results uncover the hitherto untapped potential of minimally invasive probes to study the link between mental and gut states and show the significance of deep visceral organs in the self-conscious perception of ourselves as embodied beings.

INTRODUCTION

Humans are ordinarily aware that their body is part and parcel of their self (Berlucchi and Aglioti, 2010; James, 1890; Monti et al., 2021). Physiological, clinical, and behavioral data suggest that bodily self-consciousness arises when the central nervous system integrates pieces of body-related information coming from the external and internal senses in a coherent fashion (Blanke et al., 2015; Park and Blanke, 2019). Although the contribution of sight, touch, heartbeats, and breathing to corporeal awareness is now ascertained (Ehrsson, 2007; Lenggenhager et al., 2007; Monti et al., 2020; Park et al., 2016), the role of deep, subdiaphragmatic signals is unknown. Despite their potential significance for higher-order cognitive functions (Schemann et al., 2020), organs located in the abdominal cavity, such as the stomach and the intestine, are difficult to reach and probe without relying on invasive methods (Lee et al., 2014; Saad, 2016). Gut signals are conveyed to the central nervous system via vagal and spinal afferents (Kaelberer et al., 2018; Rebollo et al., 2021; Umans and Liberles, 2018) primarily targeting the somatosensory and insular cortices. In turn, this activity is modulated by top-down control exerted by central and enteric neurons (Furness et al., 2014; Levinthal and Strick, 2020). Although the gut-brain loop has the clear homeostatic purpose of regulating food intake, it has been proposed that gut signals, once in the brain, may also influence a variety of higher-order processes, including corporeal awareness (Porciello et al., 2018; Rebollo et al., 2018).

To shed light on the visceral roots of bodily self-consciousness, we asked healthy male participants ($N = 31$) to ingest a wireless capsule (SmartPill[TM]) fitted with sensors tracking temperature, pressure, and pH values across the entire gastrointestinal tract in real-time (Saad and Hasler, 2011) (Figures 1 and 2). After ingesting the capsule, participants underwent a simplified version of the "embreathment" bodily illusion that we recently discovered (Monti et al., 2020). In particular, we administered two experimental conditions of the embreathment illusion: the *congruent* condition, which induces strong feelings of owning, controlling, and dwelling into a virtual body that looks, lays, and breathes as the physical body of the participant; and the *incongruent* condition, which induces no such feelings toward a virtual body that does not match the appearance, position, and breathing of the physical body. During each condition, we also monitored the electrogastric rhythm of our subjects through surface electrogastrography (EGG) (Yin and Chen, 2013) (Figures 1 and 3).

As the embreathment illusion relies on a combination of visual, spatial, and respiratory cues, it proved to be an appropriate method to trigger illusory feelings and gauge bodily self-consciousness at large in a controlled setting (Monti et al., 2020). To assess if and how each region of the gastrointestinal tract relates to bodily self-consciousness, we administered the illusion thrice: first when the SmartPill was in the stomach, then after the capsule entered the small bowel, and finally when it reached the large bowel (Figure 1; see STAR Methods below for details). We hypothesized that objective gut signals recorded during

[1]Sapienza, Università di Roma and Center for Life Nano- & Neuro-Science, Fondazione Istituto Italiano di Tecnologia (IIT), 00161 Rome, Italy

[2]IRCCS Fondazione Santa Lucia research hospital, 00179 Rome, Italy

[3]Department of Psychology, Sapienza, Università di Roma, 00185 Rome, Italy

[4]Lead contact

*Correspondence:
alessandro.monti@uniroma1.it (A.M.),
salvatoremaria.aglioti@uniroma1.it (S.M.A.)
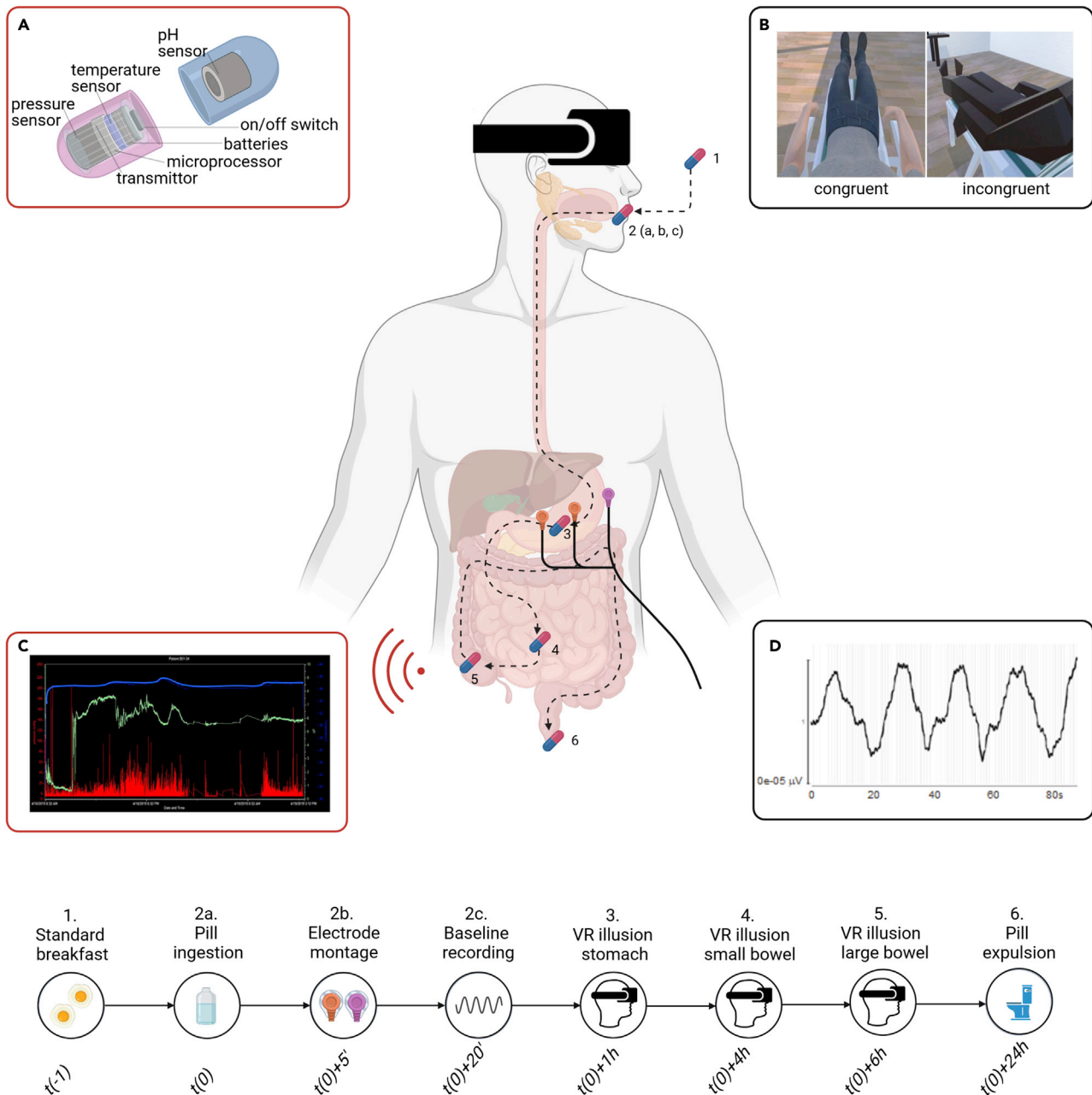https://doi.org/10.1016/j.isci.2022.105061

Figure 1. Experimental methods

Participants ingest a wireless capsule (SmartPill) fitted with sensors tracking temperature, pressure, and pH values across the entire gastrointestinal tract (A). After ingesting the capsule, participants undergo an 'embreathment' bodily illusion, embodying an avatar that either looks, lays, and breathes as the physical body of the participant (congruent condition) or not (incongruent condition) (B). During each condition, the pressure (C, red bars), pH (C, green line), and temperature (C, blue line) of the GI tract are monitored. This is done three times, as the pill moves down the three main gut regions (stomach, small bowel, and large bowel), as indicated on the timeline. Electrogastrography (EGG) is used to record gastric contractions (D). Inset A is adapted from Lee et al. (2014). For further details, see the STAR Methods section and Figures 2 and 3.

the experimental conditions would be associated with the subjective feelings of bodily self-consciousness, as gauged through a 5-item visual analog scale (VAS) questionnaire (Monti et al., 2020; see Table 1).

Specifically, we expected that the lower the gut temperature, the more the participant felt to own the congruent virtual body, analogously to what has been observed in studies linking the temperature of the skin with the
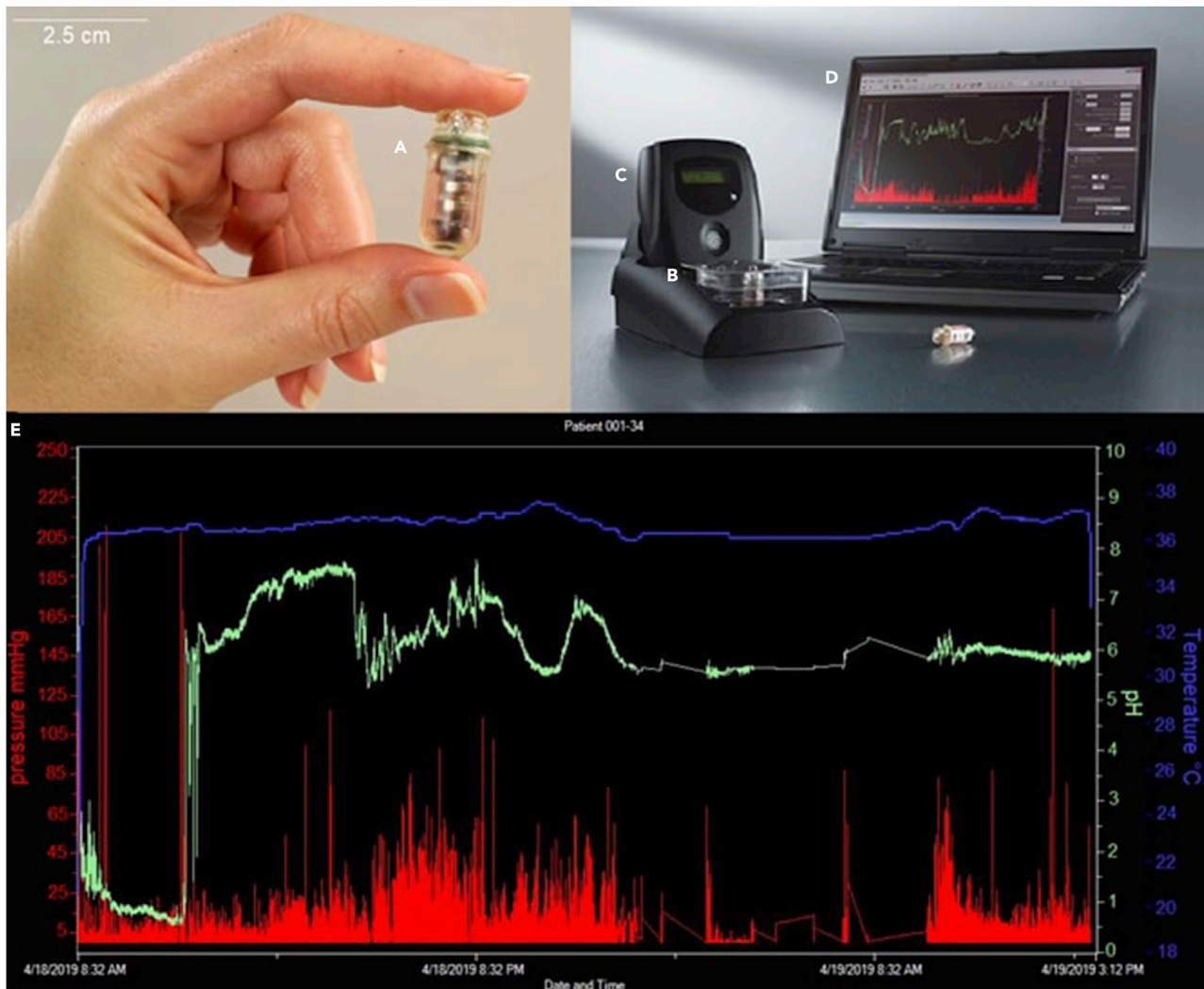
Figure 2. SmartPill apparatus

(A) capsule (2.6 × 1.3 cm). (B) pH calibration buffer solution. (C) data receiver and logger. (D) laptop. (E) graph showing pH (green line), temperature (blue line), and pressure (red bars) over time. Note the abrupt rise of the pH values in the left part of the screen, signaling the passage from the stomach to the small bowel, the slow build-up of the signal in the small bowel, and the rapid decrease marking the entrance of the pill in the large bowel. Adapted from a picture of Medtronic plc. Data shown in graph E collected from a participant in our lab.

perceived ownership of a rubber hand (Moseley et al., 2008; see also Tieri et al., 2017). In addition, we explored if also the pH and pressure of the gut covaried with feelings of owning, controlling, or dwelling in a congruent or incongruent virtual body. Moreover, as the same illusion was administered three times, we expected that the temperature, pH, and pressure of the stomach would show a stronger correlation with embodiment feelings than the equivalent parameters of the bowel, which might have been reduced by a certain degree of habituation. Finally, we wanted to compare the intra-luminal measures obtained through the SmartPill with surface electrogastrography (EGG), predicting that SmartPill parameters would provide a deeper, more nuanced insight into the physiological correlates of the embreathment illusion than the gastric rhythm alone recorded via EGG.

RESULTS

Two linear mixed-effects models measured how specific feelings of bodily self-consciousness induced by our bodily illusion (and gauged through items listed in Table 1) covaried on the one hand with the pH, pressure, and temperature values recorded by the SmartPill (Model 1); on the other hand, with gastric peak frequencies recorded by surface EGG (Model 2) (see STAR Methods for a detailed description of the models).
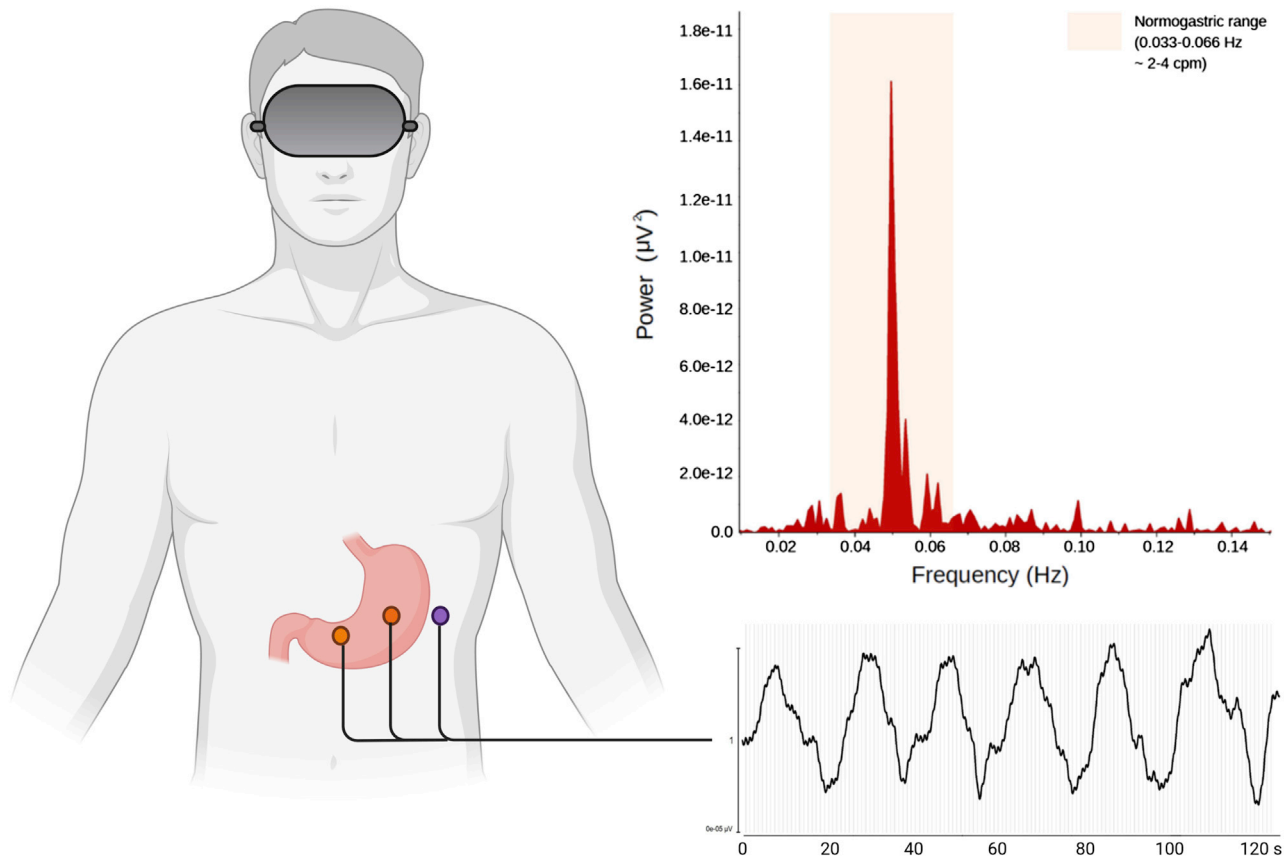
Figure 3. Electrogastrography (EGG) apparatus
1-channel EGG bipolar montage (left) with two recording electrodes (orange dots) and one ground electrode (purple dot), sample EGG recording (bottom right), and sample EGG periodogram (top right). Samples collected from a participant in our lab.

Model 1 (SmartPill) results

Type II analysis of variance of Model 1 yielded statistically significant 2-way interactions between *item* and *pressure* (F = 3.0497, p = 0.0166) and between *item* and *temperature* (F = 3.0218, p = 0.0174). Furthermore, there was a statistically significant 4-way interaction between *condition*, *item*, *gastrointestinal region*, and *pH* (F = 2.4228, p = 0.0139). The post-hoc tests of these statistically significant 2-way and 4-way interactions are presented in the following paragraphs.
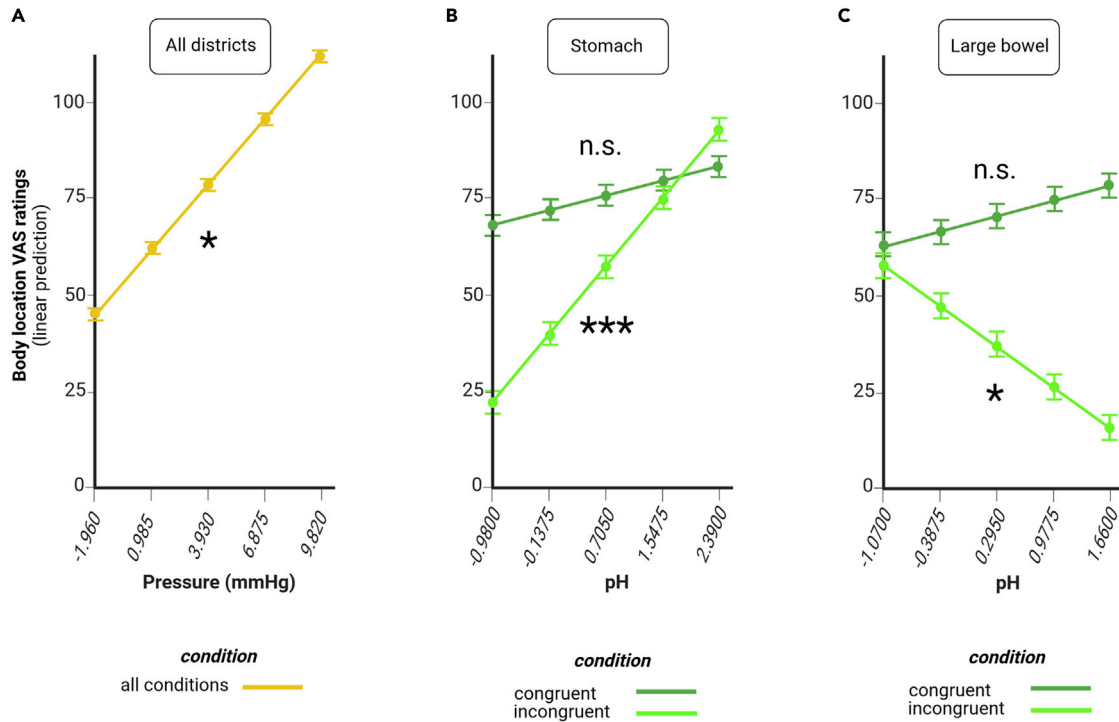
Sense of location covaries with gut pressure and pH

The higher the pressure across the gastrointestinal tract, the more our participants felt they occupied the same place of the virtual body. For each 1 mmHg increase in stomach, small bowel, or large bowel pressure, predicted VAS ratings of the feeling of being located in the virtual body went up by 5.62 $\pm$ 2.25 points (t = 2.496, p = 0.0128; Figure 4A and Table S3).

Table 1. Bodily self-consciousness questionnaire

Construct	Statement
p.body ownership	I had the feeling the virtual body/object was mine
p.body agency	I had the feeling I controlled the movements of the virtual body/object
p.body location	I had the feeling I occupied the same place of the virtual body/object
p.disembodiment	I had the feeling I had no body
p.two bodies	I had the feeling I had more than one body

p.: perceived.

SENSE OF LOCATION

A — All districts

B — Stomach

C — Large bowel

Body location VAS ratings (linear prediction) vs *Pressure (mmHg)*, *pH*, *pH*

condition: all conditions / congruent / incongruent

SENSE OF DISEMBODIMENT

D — All districts

E — Stomach

F — Small bowel

Disembodiment VAS ratings (linear prediction) vs *Temperature (°C)*, *pH*, *pH*

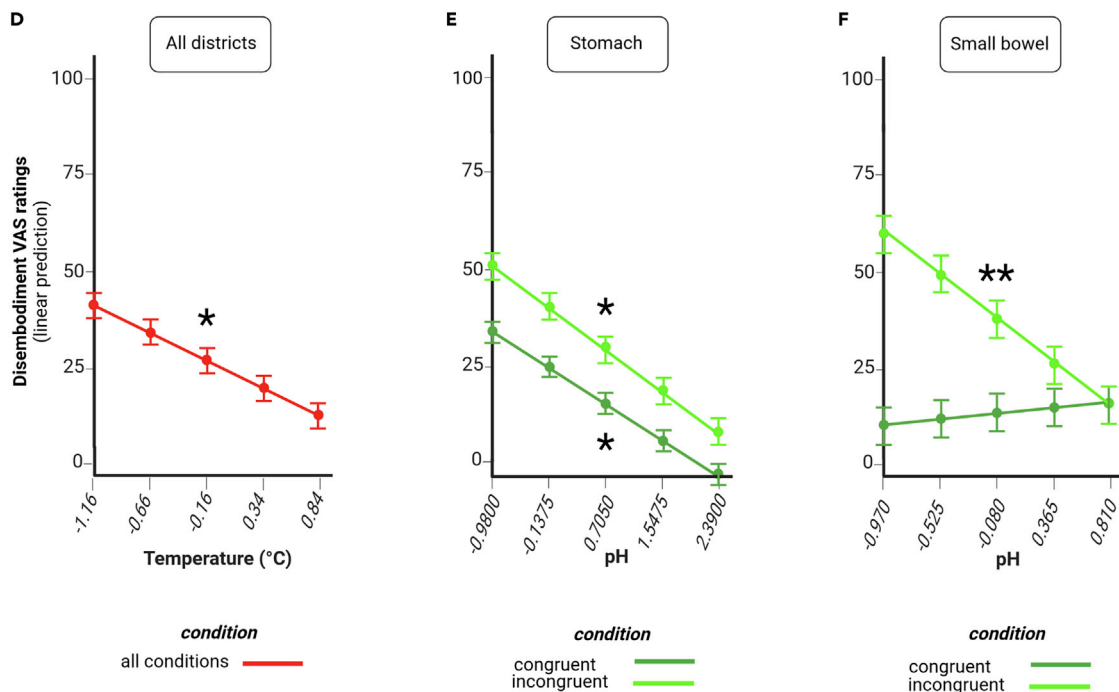condition: all conditions / congruent / incongruent

Figure 4. Gut markers of sense of location and disembodiment

Pressure (A), stomach pH (B) and large bowel pH (C) are associated with feelings of location, as assessed through visual analog scale (VAS) ratings (estimated marginal means). Temperature (D), stomach pH (E), and small bowel pH (F) are associated with feelings of disembodiment, as assessed through VAS ratings (estimated marginal means). Dots at the intersection of x and y coordinates emphasize estimated marginal means and their error bars at selected, representative values that span the range of observed values at regular intervals along a continuum. Error bars indicate standard errors. "All districts" indicates that the association holds true across all the three regions of the gastrointestinal tract we tested (stomach, small bowel, and large bowel). "Congruent condition" means that the association shown in dark green occurs when participants observe a congruent virtual body that matches their physical body. "Incongruent condition" means that the association shown in light green occurs when participants observe an incongruent virtual body that does not match their physical body. "All conditions" means that the association occurs both for congruent and incongruent condition. n.s. not significant; *p < 0.05; **p < 0.01; ***p < 0.001.

A stronger sense of location was associated also with less acidic pH of the stomach and more acidic pH of the large bowel when the virtual body did not match the real body (incongruent condition). For each 1-unit increase in stomach pH, predicted VAS ratings of being located in the incongruent virtual body increased by 21.02 ± 6.32 points ($t = 3.326$, $p < 0.001$; Figure 4B and Table S4). For each 1-unit increase in large bowel pH, the same ratings went down by 15.44 ± 6.56 points ($t = -2.355$, $p = 0.0188$; Figure 4C and Table S4).

Sense of disembodiment covaries with gut temperature and pH

We found that the higher the temperature across the gastrointestinal tract, the less our participants reported feeling disembodied when they observed a virtual body. For each 1°C increase in stomach, small bowel, or large bowel temperature, there was a 13.49 ± 5.94 point decrease in predicted VAS ratings of disembodiment ($t = -2.272$, $p = 0.0237$; Figure 4D and Table S2).

Furthermore, participants felt less disembodied also when the pH of their stomach or small intestine became less acidic. For each 1-unit increase in stomach pH, predicted VAS ratings of disembodiment fell by 11.39 ± 5.36 points when the virtual body matched the physical body of the participant (congruent condition, $t = -2.124$, $p = 0.0340$; Figure 4E and Table S4) and by 13.20 ± 6.32 points when it did not (incongruent condition, $t = -2.089$, $p = 0.0370$; Figure 4E and Table S4). Likewise, for each 1-unit increase in small bowel pH, predicted VAS ratings of disembodiment dropped by 25.00 ± 9.52 points in the incongruent condition ($t = -2.627$, $p = 0.0088$; Figure 4F and Table S4).

Sense of agency covaries with small bowel pH

The less acidic the small bowel pH, the more our participants felt they were in control of the incongruent virtual body. In the incongruent condition, for each 1-unit increase in small bowel pH, predicted VAS ratings of agency rose by 24.21 ± 9.52 points ($t = 2.545$, $p = 0.0111$; Figure 5 left and Table S4).

Other significant 3-way and 2-way interactions, as well as significant main effects, are listed in Table S1 and were not further discussed owing to the presence of the significant higher-order (2-way or 4-way) interactions described above. Of note, the *condition:item* lower-order interaction replicates previous findings on the impact of the illusion on bodily self-consciousness ratings (Monti et al., 2020).

Model 2 (electrogastrography) results

Type II ANOVA of Model 2 yielded a statistically significant 2-way interaction between *condition* and *EGG peak frequency* ($F = 4.6064$, $p = 0.033$) (Table S5). The post-hoc test of this interaction is described in the following paragraph.

All items of the bodily self-consciousness questionnaire covary with stomach peak frequency

When participants embodied a virtual body matching their real body, the higher the peak frequencies of gastric myoelectric activity, as recorded through electrogastrography (EGG), the higher the ratings across all items of the bodily self-consciousness (BSC) questionnaire. For each 0.01 Hz increase in the frequency of gastric contractions, predicted VAS ratings across the BSC questionnaire increased by 9.72 ± 3.84 points ($t = 2.534$, $p = 0.0122$; Figure 5 right and Table S6). There was also a statistically significant 2-way interaction between *condition* and *item* ($F = 15.8484$, $p < 0.001$). Other significant effects are listed in Table S5 and were not further discussed owing to the presence of significant higher-order interactions.
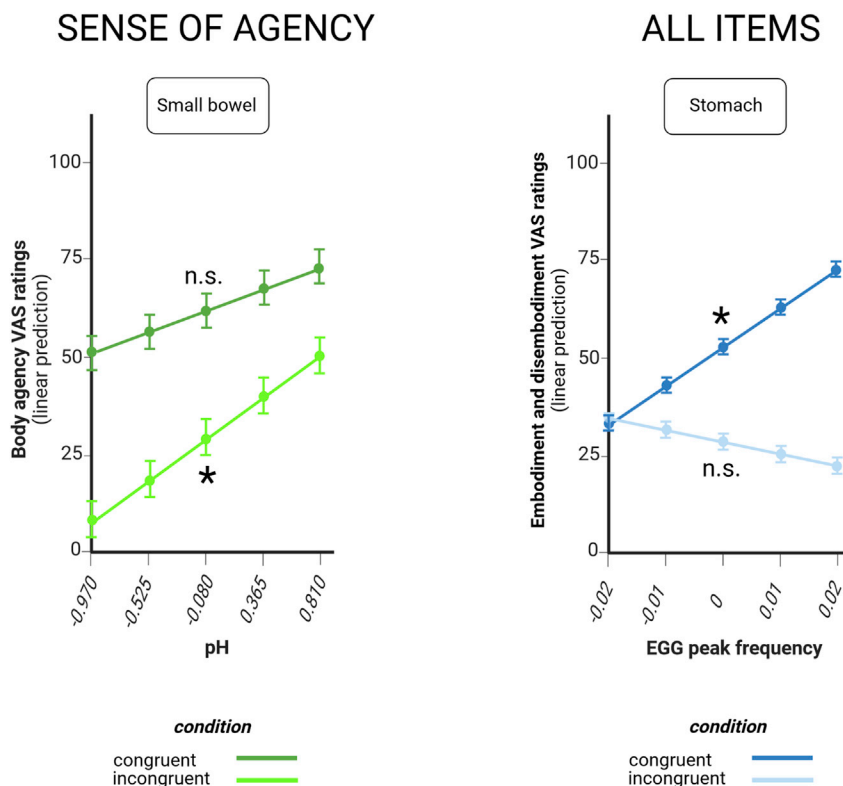
Figure 5. Gut markers of sense of agency and EGG results

Small bowel pH is associated with agency ratings (left) and EGG peak frequency is associated with all embodiment and disembodiment ratings (right).

Dots at the intersection of x and y coordinates emphasize estimated marginal means and their error bars at selected, representative values that span the range of observed values at regular intervals along a continuum. Error bars indicate standard errors. For the definition of "congruent" and "incongruent" condition, cf. Figure 2. n.s. not significant; *p < 0.05.

Interoception results

Participants displayed ordinary levels of interoception (Table S7). In particular, Shapiro-Wilk tests indicated that interoceptive sensibility, accuracy, and awareness scores did not significantly deviate from a normal distribution (interoceptive sensibility: $W = 0.969$, p = 0.565; interoceptive accuracy: $W = 0.941$, p = 0.086; interoceptive awareness: $W = 0.978$, p = 0.753).

Habituation control results

To rule out habituation effects, we performed a statistical control analysis. Specifically, a linear model tested if the illusion ratings in each condition are affected by presentation order. The results show that the number of times the illusion is presented has no statistically significant effect on ratings of any kind, across all conditions and constructs (main effect of times: $F = 0.4169$, p = 0.5187; times x condition: $F = 0.2073$, p = 0.6490; times x type of construct: $F = 0.1879$, p = 0.6648; times x condition x type of construct: $F = 0.7279$, p = 0.3938).

DISCUSSION

We capitalized on the SmartPills technology to wirelessly monitor the physiological parameters of the gastrointestinal tract in real-time while healthy subjects underwent a breathing-related bodily illusion in immersive virtual reality. This new technique allowed us to discover that specific ratings of bodily self-consciousness and specific patterns of gut activity are linked to each other. When the physiological activity of the gut increases, as signaled by the fact that the stomach becomes more acid or the bowel becomes more basic, participants tend to feel less localized in the incongruent virtual body. We speculate that signals relayed from more active organs and tissues may boost the salience and strength of own-body

representations in target cortical areas. In turn, reinforced own-body representations may reduce the feeling of being localized in an incongruent virtual body. By the same token, an uptick in gut activity should also increase the feeling of dwelling in a congruent virtual body, whose features are consistent with the representation of one's own body. Indeed, when the pressure of the gut increases, participants tend to feel as if they occupied the same place of the virtual body, although this holds true not only when the avatar is congruent, but also when it is not congruent with the real body. Hence, it may be that gut pressure activates a broader, looser "body template" compared with stomach and bowel pH.

Although we did not observe a direct link between lower gut temperature and higher ownership ratings toward the congruent virtual body as we expected, we did find that the lower the temperature, the more the participants felt disembodied. In a similar vein, the lower the small bowel pH, the higher the disembodiment ratings. As temperature scales with metabolism and small bowel works best in a high (basic) pH range, one can argue that, just like stronger gut activity may boost the own-body representation, weaker gut activity may blur this representation and make individuals feel detached from their physical body. However, in principle, during a virtual bodily illusion, also feeling detached from the *virtual* body would be enough to induce a certain degree of disembodiment. This latter, the alternative mechanism could explain why disembodiment ratings increase also when the stomach pH is low, that is, when the stomach, being more active, reinforces the own-body representation and thus makes it harder to accept the virtual body as one's own. Further research is needed to better understand the precise role of stomach pH in such a dual route to disembodiment. Nevertheless, future studies can build on these results to ascertain if feelings of disembodiment reported by patients suffering from depersonalization/derealization (Sierra and David, 2011), Cotard's syndrome (Berrios and Luque, 1995), and eating disorders (Fuchs, 2021) are related to impaired (processing of) gut temperature or acidity.

Overall, the fact that gut activity tends to scale with embodiment is consistent with analogous trends observed in other physiological domains, including respiration (Monti et al., 2020), histamine reactivity (Barnsley et al., 2011), skin temperature (Tieri et al., 2017) and skin conductance (Armel and Ramachandran, 2003; Mello et al., 2021; Tieri et al., 2015). On this point, compared to all other internal or external sources of information about one's own body, signals coming from the stomach and the bowel are a particularly steady source of bodily self-consciousness, as they change at a much slower pace and never cease to relay information to the central nervous system. However, in this experiment, we adopted an associational approach to link embreathment-evoked changes in gut physiology to perceptual measures of bodily self-consciousness. As such, these associations cannot confirm that the gut physiology changes were the driving factors. Hence, it may also be that physiological activation is an effect, rather than a cause, of higher embodiment and lower disembodiment. Nevertheless, as two seemingly independent readouts—gut physiological signals and embodiment—are in fact related to each other, they can be putatively considered to be elements of a feedback loop involving the brain and body. To shed light on causality, new experimental paradigms could pair smart pills with protocols that stimulate or inhibit the activity of the stomach and the bowel, e.g. presenting pictures (Zhou et al., 2004), evoking food-related thoughts (Zhou and Hu, 2007) or electrically stimulating the vagal afferents (Hong et al., 2019; Teckentrup et al., 2020). Computational models of predictive processing within the framework of a clinical trial (Khalsa et al., 2022) may also prove useful in this regard.

In keeping with signals recorded by the SmartPill, also electrogastrographic (EGG) data show that a surge in the physiological activity of the stomach, as measured through EGG peak frequency, is tied to a surge in bodily self-consciousness feelings toward a congruent avatar. Of note, whilst gut pressure, pH, and temperature are differentially tied to specific facets of bodily self-consciousness, an increase in EGG peak frequency is correlated with a generalized increase of all questionnaire ratings, including both embodiment and disembodiment items. This suggests that gastric rhythms, too, can play a significant if less specific role in the experience of bodily self-consciousness. This is further corroborated by recent evidence, indicating that a lower gastric-alpha phase-amplitude coupling is associated with a more negative body image (Todd et al., 2021). New research may build on these results to modulate the perception of one's own body through selective changes in gastric frequencies or in other physiological parameters of the gut.

Although we expected that correlations between physiological parameters and embodiment ratings would be stronger in the stomach than in the subsequent parts of the gastrointestinal tract, results obtained in the small and large bowel suggest that the contribution of the lower gut to bodily self-consciousness is robust

enough to resist serial effects. Monitoring the largely independent changes that occur not just in the stomach, but also in the intestines, SmartPills thus provide a heretofore unexamined signal that is indicative, if not necessarily fully reflective, of the status of the whole gut. Indeed, although the current technology does not offer a picture of the whole gut at a glance, as signals from each gut segment are recorded sequentially rather than simultaneously, tracking GI parameters while repeating the embreathment illusion yields a nuanced, comprehensive description of the links between gut physiology and the bodily self. Hence, ingestible capsules offer researchers a new method to gauge the correlation between gut states and mental states with unprecedented detail. Together with other ingestibles (Abramson et al., 2020; Gibson and Burgell, 2018; Mayeli et al., 2021; Mimee et al., 2018; Smith et al., 2021), smart pills could become a particularly valuable, minimally invasive tool for assessing also other important psychological constructs that may be rooted in gastrointestinal physiology, from emotions (Vianna and Tranel, 2006) to moral disgust (Eskine et al., 2011; Rozin et al., 2009).

Limitations of the study

Previous research suggests that there might be sex differences in interoceptive abilities. In particular, men seem to pay less attention to bodily signals than women (Grabauskaitė et al., 2017), while slightly outperforming them in cardiac (Grabauskaitė et al., 2017; Harver et al., 1993) if not gastric (Prentice and Murphy, 2022) interoception accuracy tasks, and displaying a more stable EGG frequency (Tolj et al., 2007). Hence, recruiting only male participants allowed us to test how gastrointestinal signals are related to bodily self-consciousness in a more homogeneous sample. Nevertheless, we are aware that future experiments should involve a larger sample of participants of both sexes to increase the generalizability of the present findings. Finally, although the ingestible device is minimally invasive, its dimensions (2.6 × 1.3 cm) and sampling rate (1 data point/500 ms) are sub-optimal. Ongoing advances in pill technology may lead to smaller and hence easier to swallow capsules that will be fitted with more efficient sensors to gather a higher amount of data in a shorter time. Such innovative ingestibles will further improve our understanding of the connection between our gut and our bodily self.

STAR★METHODS

Detailed methods are provided in the online version of this paper and include the following:

- KEY RESOURCES TABLE
- RESOURCE AVAILABILITY
  - Lead contact
  - Materials availability
  - Data and code availability
- EXPERIMENTAL MODEL AND SUBJECT DETAILS
  - Participants
- METHOD DETAILS
  - Materials
  - Data collection procedure
- QUANTIFICATION AND STATISTICAL ANALYSIS
  - SmartPill data pre-processing
  - EGG data pre-processing
  - VAS questionnaire data pre-processing
  - Statistical data analysis

SUPPLEMENTAL INFORMATION

Supplemental information can be found online at https://doi.org/10.1016/j.isci.2022.105061.

AUTHOR CONTRIBUTIONS

Conceptualization and methodology: AM, GP, MSP, SMA. Data curation, formal analysis, investigation: AM, GP, MSP. Funding acquisition, project administration, resources, supervision: SMA. Software, visualization, writing – original draft: AM. Writing – review & editing: AM, GP, MSP, SMA.

DECLARATION OF INTERESTS

The authors declare no competing interests.

REFERENCES

Abramson, A., Dellal, D., Kong, Y.L., Zhou, J., Gao, Y., Collins, J., Tamang, S., Wainer, J., McManus, R., Hayward, A., et al. (2020). Ingestible transiently anchoring electronics for microstimulation and conductive signaling. Sci. Adv. 6, eaaz0127. https://doi.org/10.1126/sciadv.aaz0127.

Al-Shboul, O.A. (2013). The importance of interstitial cells of cajal in the gastrointestinal tract. Saudi J. Gastroenterol. 19, 3–15. https://doi.org/10.4103/1319-3767.105909.

Armel, K.C., and Ramachandran, V.S. (2003). Projecting sensations to external objects: evidence from skin conductance response. Proc. Biol. Sci. 270, 1499–1506. https://doi.org/10.1098/rspb.2003.2364.

Barnsley, N., McAuley, J.H., Mohan, R., Dey, A., Thomas, P., and Moseley, G.L. (2011). The rubber hand illusion increases histamine reactivity in the real arm. Curr. Biol. 21, R945–R946. https://doi.org/10.1016/j.cub.2011.10.039.

Bates, D., Mächler, M., Bolker, B., and Walker, S. (2015). Fitting linear mixed-effects models using lme4. J. Stat. Softw. 67, 1–48. https://doi.org/10.18637/jss.v067.i01.

Berlucchi, G., and Aglioti, S.M. (2010). The body in the brain revisited. Exp. Brain Res. 200, 25–35. https://doi.org/10.1007/s00221-009-1970-7.

Berrios, G.E., and Luque, R. (1995). Cotard's syndrome: analysis of 100 cases. Acta Psychiatr. Scand. 91, 185–188. https://doi.org/10.1111/j.1600-0447.1995.tb09764.x.

Blanke, O., Slater, M., and Serino, A. (2015). Behavioral, neural, and computational principles of bodily self-consciousness. Neuron 88, 145–166. https://doi.org/10.1016/j.neuron.2015.09.029.

Calì, G., Ambrosini, E., Picconi, L., Mehling, W.E., and Committeri, G. (2015). Investigating the relationship between interoceptive accuracy, interoceptive awareness, and emotional susceptibility. Front. Psychol. 6, 1202. https://doi.org/10.3389/fpsyg.2015.01202.

Craig, A.D. (2002). How do you feel? Interoception: the sense of the physiological condition of the body. Nat. Rev. Neurosci. 3, 655–666. https://doi.org/10.1038/nrn894.

Ehrsson, H.H. (2007). The experimental induction of out-of-body experiences. Science 317, 1048. https://doi.org/10.1126/science.1142175.

Eskine, K.J., Kacinik, N.A., and Prinz, J.J. (2011). A bad taste in the mouth: gustatory disgust influences moral judgment. Psychol. Sci. 22, 295–299. https://doi.org/10.1177/0956797611398497.

Fuchs, T. (2021). The disappearing body: anorexia as a conflict of embodiment. Eat. Weight Disord. 27, 109–117. https://doi.org/10.1007/s40519-021-01122-7.

Furness, J.B., Callaghan, B.P., Rivera, L.R., and Cho, H.-J. (2014). The enteric nervous system and gastrointestinal innervation: integrated local and central control. In Microbial Endocrinology: The Microbiota-Gut-Brain Axis in Health and Disease, Advances in Experimental Medicine and Biology, M. Lyte and J.F. Cryan, eds. (Springer), pp. 39–71. https://doi.org/10.1007/978-1-4939-0897-4_3.

Garfinkel, S.N., Seth, A.K., Barrett, A.B., Suzuki, K., and Critchley, H.D. (2015). Knowing your own heart: distinguishing interoceptive accuracy from interoceptive awareness. Biol. Psychol. 104, 65–74. https://doi.org/10.1016/j.biopsycho.2014.11.004.

Gelman, A., and Hill, J. (2007). Data Analysis Using Regression and Multilevel/Hierarchical Models (Cambridge University Press).

Gibson, P.R., and Burgell, R.E. (2018). Illuminating dark depths. Science 360, 856–857. https://doi.org/10.1126/science.aat8658.

Grabauskaitė, A., Baranauskas, M., and Griškova-Bulanova, I. (2017). Interoception and gender: what aspects should we pay attention to? Conscious. Cogn. 48, 129–137. https://doi.org/10.1016/j.concog.2016.11.002.

Harrison, X.A., Donaldson, L., Correa-Cano, M.E., Evans, J., Fisher, D.N., Goodwin, C.E.D., Robinson, B.S., Hodgson, D.J., and Inger, R. (2018). A brief introduction to mixed effects modelling and multi-model inference in ecology. PeerJ 6, e4794. https://doi.org/10.7717/peerj.4794.

Harver, A., Katkin, E.S., and Bloch, E. (1993). Signal-detection outcomes on heartbeat and respiratory resistance detection tasks in male and

female subjects. Psychophysiology 30, 223–230. https://doi.org/10.1111/j.1469-8986.1993.tb03347.x.

Hayes, M.H., and Patterson, D.G. (1921). Experimental developement of the graphics rating method. Physiol Bull 18, 98–99.

Hong, G.-S., Pintea, B., Lingohr, P., Coch, C., Randau, T., Schaefer, N., Wehner, S., Kalff, J.C., and Pantelis, D. (2019). Effect of transcutaneous vagus nerve stimulation on muscle activity in the gastrointestinal tract (transVaGa): a prospective clinical trial. Int. J. Colorectal Dis. 34, 417–422. https://doi.org/10.1007/s00384-018-3204-6.

Huizinga, J.D., and Lammers, W.J.E.P. (2009). Gut peristalsis is governed by a multitude of cooperating mechanisms. Am. J. Physiol. Gastrointest. Liver Physiol. 296, G1–G8. https://doi.org/10.1152/ajpgi.90380.2008.

James, W. (1890). The Principles of Psychology (Holt).

Johnson, P.C. (2014). Extension of Nakagawa & Schielzeth's R2GLMM to random slopes models. Methods Ecol. Evol. 5, 944–946. https://doi.org/10.1111/2041-210X.12225.

Kaelberer, M.M., Buchanan, K.L., Klein, M.E., Barth, B.B., Montoya, M.M., Shen, X., and Bohórquez, D.V. (2018). A gut-brain neural circuit for nutrient sensory transduction. Science 361, eaat5236. https://doi.org/10.1126/science.aat5236.

Kenward, M.G., and Roger, J.H. (1997). Small sample inference for fixed effects from restricted maximum likelihood. Biometrics 53, 983–997. https://doi.org/10.2307/2533558.

Khalsa, S.S., Berner, L.A., and Anderson, L.M. (2022). Gastrointestinal interoception in eating disorders: charting a new path. Curr. Psychiatry Rep. 24, 47–60. https://doi.org/10.1007/s11920-022-01318-3.

K.L. Koch, and R.M. Stern, eds. (2003). Handbook of Electrogastrography (Oxford University Press).

Kuznetsova, A., Brockhoff, P.B., and Christensen, R.H.B. (2017). **lmerTest** package: tests in linear mixed effects models. J. Stat. Soft. 82. https://doi.org/10.18637/jss.v082.i13.

Lee, Y.Y., Erdogan, A., and Rao, S.S.C. (2014). How to assess regional and whole gut transit time with wireless motility capsule. J. Neurogastroenterol. Motil. 20, 265–270. https://doi.org/10.5056/jnm.2014.20.2.265.

Lenggenhager, B., Tadi, T., Metzinger, T., and Blanke, O. (2007). Video ergo sum: manipulating bodily self-consciousness. Science 317, 1096–1099. https://doi.org/10.1126/science.1143439.

Levinthal, D.J., and Strick, P.L. (2020). Multiple areas of the cerebral cortex influence the stomach. Proc. Natl. Acad. Sci. USA 117, 13078–13083. https://doi.org/10.1073/pnas.2002737117.

Longo, M.R., Schüür, F., Kammers, M.P.M., Tsakiris, M., and Haggard, P. (2008). What is embodiment? A psychometric approach. Cognition 107, 978–998. https://doi.org/10.1016/j.cognition.2007.12.004.

Luke, S.G. (2017). Evaluating significance in linear mixed-effects models in R. Behav. Res. Methods 49, 1494–1502. https://doi.org/10.3758/s13428-016-0809-y.

Mayeli, A., Zoubi, O.A., White, E.J., Chappelle, S., Kuplicki, R., Smith, R., Feinstein, J.S., Bodurka, J., Paulus, M.P., and Khalsa, S.S. (2021). Neural indicators of human gut feelings. Preprint at bioRxiv. https://doi.org/10.1101/2021.02.11.430867.

Mello, M., Fusaro, M., Tieri, G., and Aglioti, S.M. (2021). Wearing same- and opposite-sex virtual bodies and seeing them caressed in intimate areas. Q. J. Exp. Psychol. 75, 461–474. https://doi.org/10.1177/17470218211031557.

Mimee, M., Nadeau, P., Hayward, A., Carim, S., Flanagan, S., Jerger, L., Collins, J., McDonnell, S., Swartwout, R., Citorik, R.J., et al. (2018). An ingestible bacterial-electronic system to monitor gastrointestinal health. Science 360, 915–918. https://doi.org/10.1126/science.aas9315.

Monti, A., Porciello, G., Panasiti, M.S., and Aglioti, S.M. (2021). The inside of me: interoceptive constraints on the concept of self in neuroscience and clinical psychology. Psychol. Res. https://doi.org/10.1007/s00426-021-01477-7.

Monti, A., Porciello, G., Tieri, G., and Aglioti, S.M. (2020). The "embreathment" illusion highlights the role of breathing in corporeal awareness. J. Neurophysiol. 123, 420–427. https://doi.org/10.1152/jn.00617.2019.

Moseley, G.L., Olthof, N., Venema, A., Don, S., Wijers, M., Gallace, A., and Spence, C. (2008). Psychologically induced cooling of a specific body part caused by the illusory ownership of an artificial counterpart. Proc. Natl. Acad. Sci. USA 105, 13169–13173. https://doi.org/10.1073/pnas.0803768105.

Oostenveld, R., Fries, P., Maris, E., and Schoffelen, J.-M. (2011). FieldTrip: open source software for advanced analysis of MEG, EEG, and invasive electrophysiological data. Comput. Intell. Neurosci. 2011, 156869. https://doi.org/10.1155/2011/156869.

Park, H.-D., Bernasconi, F., Bello-Ruiz, J., Pfeiffer, C., Salomon, R., and Blanke, O. (2016). Transient modulations of neural responses to heartbeats covary with bodily self-consciousness. J. Neurosci. 36, 8453–8460. https://doi.org/10.1523/JNEUROSCI.0311-16.2016.

Park, H.-D., and Blanke, O. (2019). Coupling inner and outer body for self-consciousness. Trends Cogn. Sci. 23, 377–388. https://doi.org/10.1016/j.tics.2019.02.002.

Porciello, G., Monti, A., and Aglioti, S.M. (2018). How the stomach and the brain work together at rest. Elife 7, e37009. https://doi.org/10.7554/eLife.37009.

Prentice, F., and Murphy, J. (2022). Sex differences in interoceptive accuracy: a meta-analysis. Neurosci. Biobehav. Rev. 132, 497–518. https://doi.org/10.1016/j.neubiorev.2021.11.030.

Rebollo, I., Devauchelle, A.-D., Béranger, B., and Tallon-Baudry, C. (2018). Stomach-brain synchrony reveals a novel, delayed-connectivity resting-state network in humans. Elife 7, e33321. https://doi.org/10.7554/eLife.33321.

Rebollo, I., Wolpert, N., and Tallon-Baudry, C. (2021). Brain–stomach coupling: Anatomy, functions, and future avenues of research. Current Opinion in Biomedical Engineering 18, 100270. https://doi.org/10.1016/j.cobme.2021.100270.

Rozin, P., Haidt, J., and Fincher, K. (2009). From oral to moral. Science 323, 1179–1180. https://doi.org/10.1126/science.1170492.

Saad, R.J. (2016). The wireless motility capsule: a one-stop shop for the evaluation of GI motility disorders. Curr. Gastroenterol. Rep. 18, 14. https://doi.org/10.1007/s11894-016-0489-x.

Saad, R.J., and Hasler, W.L. (2011). A technical review and clinical assessment of the wireless motility capsule. Gastroenterol. Hepatol. 7, 795–804.

Satterthwaite, F.E. (1941). Synthesis of variance. Psychometrika 6, 309–316.

Schandry, R. (1981). Heart beat perception and emotional experience. Psychophysiology 18, 483–488.

Schemann, M., Frieling, T., and Enck, P. (2020). To learn, to remember, to forget—how smart is the gut? Acta Physiol. 228, e13296. https://doi.org/10.1111/apha.13296.

Sierra, M., and David, A.S. (2011). Depersonalization: a selective impairment of self-awareness. Conscious. Cogn. 20, 99–108. https://doi.org/10.1016/j.concog.2010.10.018.

Smith, R., Mayeli, A., Taylor, S., Al Zoubi, O., Naegele, J., and Khalsa, S.S. (2021). Gut inference: a computational modelling approach. Biol. Psychol. 164, 108152. https://doi.org/10.1016/j.biopsycho.2021.108152.

Teckentrup, V., Neubert, S., Santiago, J.C.P., Hallschmid, M., Walter, M., and Kroemer, N.B. (2020). Non-invasive stimulation of vagal afferents reduces gastric frequency. Brain Stimul. 13, 470–473. https://doi.org/10.1016/j.brs.2019.12.018.

Tieri, G., Gioia, A., Scandola, M., Pavone, E.F., and Aglioti, S.M. (2017). Visual appearance of a virtual upper limb modulates the temperature of the real hand: a thermal imaging study in Immersive Virtual Reality. Eur. J. Neurosci. 45, 1141–1151. https://doi.org/10.1111/ejn.13545.

Tieri, G., Tidoni, E., Pavone, E.F., and Aglioti, S.M. (2015). Body visual discontinuity affects feeling of ownership and skin conductance responses. Sci. Rep. 5, 17139. https://doi.org/10.1038/srep17139.

Todd, J., Cardellicchio, P., Swami, V., Cardini, F., and Aspell, J.E. (2021). Weaker implicit interoception is associated with more negative body image: evidence from gastric-alpha phase amplitude coupling and the heartbeat evoked potential. Cortex 143, 254–266. https://doi.org/10.1016/j.cortex.2021.07.006.

Tolj, N., Luetić, K., Schwarz, D., Bilić, A., Jurčić, D., and Gabrić, M. (2007). The impact of age, sex, body mass index and menstrual cycle phase on gastric myoelectrical activity characteristics in a healthy Croatian population. Coll. Antropol. 31, 955–962.

Umans, B.D., and Liberles, S.D. (2018). Neural sensing of organ volume. Trends Neurosci. 41, 911–924. https://doi.org/10.1016/j.tins.2018.07.008.

Vianna, E.P.M., and Tranel, D. (2006). Gastric myoelectrical activity as an index of emotional arousal. Int. J. Psychophysiol. 61, 70–76. https://doi.org/10.1016/j.ijpsycho.2005.10.019.

Yin, J., and Chen, J.D.Z. (2013). Electrogastrography: methodology, validation and Applications. J. Neurogastroenterol. Motil. 19, 5–17. https://doi.org/10.5056/jnm.2013.19.1.5.

Zhou, R., and Hu, S. (2007). Effects of imagining eating favorable and unfavorable foods on gastric motility indexed by electrogastrographic (EGG) activities. Percept. Mot. Skills 103, 829–833. https://doi.org/10.2466/PMS.103.7.829-833.

Zhou, R., Luo, Y., and Hu, S. (2004). Effects of viewing pleasant and unpleasant photographs on gastric motility indexed by electrogastrographic (EGG) Activities. Percept. Mot. Skills 99, 785–789. https://doi.org/10.2466/pms.99.3.785-789.

STAR★METHODS

KEY RESOURCES TABLE

REAGENT or RESOURCE	SOURCE	IDENTIFIER
Deposited data		
Raw data	This study	OSF project link
Software and algorithms		
Unity 5.6.0f3	Unity Technologies Inc	unity3d.com/get-unity
3ds Max	Autodesk Inc.	autodesk.eu/products/3ds-max
R 3.6.1	The R Foundation	r-project.org
FieldTrip	Robert Oostenveld,	fieldtriptoolbox.org
	Pascal Fries, Eric Maris,	
	Jan-Mathijs Schoffelen	

RESOURCE AVAILABILITY

Lead contact

Further information and requests for resources should be directed to and will be fulfilled by the lead contact, Alessandro Monti (alessandro.monti.0791@gmail.com).

Materials availability

This study did not generate any new unique reagents.

Data and code availability

- The experimental data that support the findings of this study are available in our Open Science Foundation (OSF) project at https://osf.io/wecta/?view_only=45e1a9e30c2a47efa82c10161b70b732.

- The experiment code and the analysis code are available in our OSF project at https://osf.io/wecta/?view_only=45e1a9e30c2a47efa82c10161b70b732.

- The study has not been preregistered. Any additional information required to reanalyse the data reported in this paper is available from the lead contact upon request.

EXPERIMENTAL MODEL AND SUBJECT DETAILS

Participants

Thirty-one healthy men aged 20–30 years (M = 24.42, SD = 2.8) took part in the study after giving their informed consent. The study was reviewed and approved by the Fondazione Santa Lucia ethics committee. All subjects were naive to the purpose of the research and were paid for their participation. No subject had a history of psychiatric or neurologic disorders. A detailed screening procedure ensured that all participants were eligible for ingesting the SmartPill[TM] without any known contraindication (history of gastric bezoars; history of any abdominal/pelvic surgery within the previous three months; swallowing disorders; suspected or known strictures, fistulas, or physiological/mechanical obstruction within the gastro-intestinal tract; dysphagia to food or pills; Crohn's disease or diverticulitis; body mass index ≥40; and cardiac pacemakers or defibrillators (Saad, 2016).

METHOD DETAILS

Materials

SmartPill[TM]

The gastro-intestinal milieu of each participant was monitored through a SmartPill[TM] (SmartPill Motility Testing System, Medtronic plc). SmartPills are light, single-use, orally ingestible capsules (length: 26 mm; width: 13 mm; weight: 4.5 g). Each pill consists of a polyurethane shell fitted with a long-lasting battery (>5 days), a transmitter (broadcast frequency: 434.2 MHz), and internal sensors probing temperature

(range: 20–42°C; accuracy: $\pm$ 1°C), intra-luminal pressure (range: 0–350 mmHg; accuracy: $\pm$ 5 mmHg in the 0–99 mmHg sub-range, $\pm$ 10% of applied pressure in the 100–350 mmHg sub-range) and pH (range: 1–9; accuracy: $\pm$ 0.5 pH units) of the gastro-intestinal (GI) tract (Figure 2A).

Before being ingested, the pill is activated through a magnetic fixture and the pH sensor is calibrated through a buffer solution (Figure 2B). After ingestion, the capsule samples temperature data every 20 s, pressure every 0.5 s, and pH every 5 s for the first 24 h; sampling frequencies are halved thereafter. The pill transmitter wirelessly sends these data to an external radio receiver (operating range: $\sim$ 1.5 m), which can be either docked in a dedicated station or comfortably fastened to a belt worn by the participant (Figure 2C).

Combining pH, pressure, and temperature information, the MotiliGI software (Medtronic plc) univocally identifies the specific segment of the GI tract in which the pill is located at a given time. The software takes an abrupt increase of $\geq$2 pH units as a sign that the pill left the stomach and entered the small intestine. Likewise, the software interprets a subsequent gradual decrease of $\geq$1 pH unit for at least 10 consecutive minutes as a sign that the pill left the small intestine and entered the large intestine (Figure 2D). In our sample, 30 out of 31 subjects displayed a pH increase and decrease as expected, while for the remaining subject the software was still able to localize the GI districts that the pill went through based on pressure, temperature, and time data.

Electrogastrography (EGG)

Electrogastrographic (EGG) recordings were used as a measure of gastric contractions. EGG records the electrophysiological activity of a selected cluster of cells at the junction of the enteric nervous system with the stomach – the so-called interstitial cells of Cajal (ICC). ICC act as pacemakers of stomach contractions by generating and propagating electric slow waves that have a normal frequency of 0.05 Hz, i.e. 3 cycles/minute (Al-Shboul, 2013; Huizinga and Lammers, 2009). In healthy subjects, each slow wave is coupled to a gastric contraction (Yin and Chen, 2013).

Slow wave electrical signals were recorded through a standard 1-channel EGG bipolar montage (Yin and Chen, 2013) with 3 pre-gelled disposable Ag/AgCl electrodes. Participants were instructed to lie supine on a deck chair, then their abdominal skin was accurately cleansed to reduce impedance. The first recording electrode was placed halfway between their xyphoid and their umbilicus, while the second recording electrode lay 5 cm up and 5 cm to the left of the first (taking the left side of participants as a reference) and the ground electrode lay on the left costal margin (Figure 3).

Immersive virtual reality

The immersive virtual reality apparatus for the embreathment illusion (Monti et al., 2020) included a virtual scenario designed in 3DS Max 2015 (Autodesk Inc) and Unity 2017.1 (Unity Technologies SF). The scenario was broadcasted to a VIVE headset (HTC Corp., 6 degrees of freedom, field of view: $\sim$110°, resolution: 2160 $\times$ 1200 (1080 $\times$ 1200 per eye, aspect ratio 9:5), refresh rate: 90 Hz) and consisted of a life-size room in which a virtual body (avatar) lay on a deck chair.

In the *congruent* condition, the avatar was seen from a first-person perspective, had a human-like appearance, and breathed as the participant, i.e. it inspired when the participant inspired and expired when the participant expired, in real time. The exact alignment of real and virtual breathing was obtained through a customized VIVE sensor (Video S1) that mapped real, respiration-induced belly movements onto the virtual body with sub-millimetric precision (error $<10^{-3}$ m).

In the *incongruent* condition, the avatar was seen from a third-person perspective, had an object-like wooden appearance, and breathed in anti-phase with the participant, i.e. it expired when the participant inspired and vice versa, in real time. The same VIVE sensor described above was adopted also in this condition, although in this case the y axis of the sensor was mapped in a reverse fashion onto the virtual body to further enhance the incongruity effect.

A custom graphical user interface (GUI) was embedded in the virtual scenario, allowing participants to answer some questions relative to bodily self-consciousness (see below) at the end of each condition. For a detailed footage of the immersive virtual reality experience, please see Video S1.

Measures of bodily self-consciousness

At the end of each virtual reality condition, we administered a customized bodily self-consciousness questionnaire (Monti et al., 2020; cf. Longo et al., 2008) consisting of five different visual analogue scales (VAS; Hayes and Paterson, 1921). In each scale, participants indicated how much they agreed with a statement by using a joystick to select a point on a line ranging from complete disagreement (leftmost point) to complete agreement (rightmost point). Table 1 shows the complete list of statements, while Figure S1 contains a box-plot of the individual responses.

Measures of interoception

We also measured objective (Schandry, 1981) and subjective (Calì et al., 2015) levels of interoception, i.e. how participants perceived their inner physiological signals (Craig, 2002) (see Table S7 for descriptive statistics).

Interoceptive sensibility, that is, the participants' subjective, self-reported ability to monitor interoceptive signals (Garfinkel et al., 2015), was measured through the Italian version of the Multidimensional Assessment of Interoceptive Awareness (MAIA) (Calì et al., 2015), a list of 32 questions sampling how much each participant is aware of their physiological state. In particular, the average of three MAIA subscales (*Noticing*, *Attention Regulation*, and *Body Listening*) was taken as a proxy of interoceptive sensibility. Responses were provided with a 6-point Likert scale.

Interoceptive accuracy, that is, the participants' objective performance at perceiving interoceptive signals (Garfinkel et al., 2015), was assessed via Schandry's heartbeat counting task (Schandry, 1981). Subjects were asked to report the number of heartbeats they perceived in four different time windows (25, 35, 45, 100 s) without guessing or relying on external cues (e.g. taking their own pulse). Meanwhile, EGG electrodes were used to pick objective electrocardiographic (EKG) signals. Raw EKG recordings were processed in LabChart to detect the QRS complex associated with each heartbeat and thus compute the actual number of heartbeats for each time window. These objective data were then paired with self-reported numbers of heartbeats for each time window to calculate an interoceptive accuracy score for each participant ranging from 0 (not accurate at all) to 1 (perfect accuracy).

Interoceptive awareness, that is, the participants' confidence in how well they fared in the heartbeat counting task, was gauged through a visual analogue scale (VAS) that ranged from 0 (indicating participants believed their performance was extremely poor) to 100 (indicating participants believed their performance was extremely good).

Data collection procedure

To ensure that the data gathered by the SmartPill were as reliable as possible, subjects were instructed to discontinue any medication that could interfere with pH values and gastro-intestinal motility (Saad, 2016). Specifically, we checked that none of the participants was assuming any: i) proton pump inhibitors in the seven days before the experiment; ii) antihistamines, prokinetics, antiemetics, anticholinergics, antidiarrheals, narcotic analgesics, and non-steroidal anti-inflammatory drugs in the three days before the experiment; iii) laxatives in the two days before the experiment. Participants were instructed not to take antacids and any alcohol the day before the experiment. Eight hours before the experiment, they also stopped eating and smoking.

The day of the experiment, participants came to the laboratory, filled in the informed consent form, and ate a standardized ∼260 kcal breakfast consisting of egg whites (120 g), two slices of bread, and jam (30 g) to make sure that gastro-intestinal transit times of the SmartPill were not affected by meal variability. Meanwhile, we activated the capsule through a magnetic fixture and calibrated the capsule pH sensor (see Materials above, section *SmartPill*).

After calibration was complete, the pill started transmitting data to the radio receiver. Data came with a relative time stamp indicating the number of seconds elapsed from calibration, but no absolute time reference. To overcome this issue, we synchronized calibration with an external clock that provided us with the required absolute time frame. At that point, participants swallowed the SmartPill while drinking a glass of water (120 mL). A medical doctor supervised the ingestion procedure to help in case of swallowing problems. All subjects ingested the pill without any trouble.

After the ingestion, participants fastened the receiver around their belt and lay supine on a deck chair. This allowed the experimenters to place EGG electrodes according to the montage described above (see Materials, section *Electrogastrography*). When the whole apparatus was in place, we recorded a 15-min resting-state SmartPill/EGG baseline session in which participants were instructed to relax and keep their eyes open. Then, we perused real-time pH data displayed on the receiver to make sure that the capsule was working and actually lay in the stomach, as signaled by a highly acidic pH ($\sim$1–2). After this requirement was fulfilled, we administered a simplified version of the embreathment illusion (Monti et al., 2020) delivered through a virtual reality headset and a customized breathing sensor (see Materials, section *Immersive virtual reality*). Both the *congruent* and the *incongruent* condition of the illusion (see above) lasted for 240 s. Participants were asked to pay attention to the trunk of the avatar and then complete the bodily self-consciousness questionnaire at the end of each condition (see Materials, section *Measures of bodily self-consciousness*). To control for confounding due to order and carryover effects, the items of the questionnaire were randomised, the order of experimental conditions was counterbalanced across participants, and conditions were interspersed with 5′ washout pauses. Throughout each experimental condition, the receiver logged SmartPill data about the pressure, temperature, and pH of the stomach, while a dedicated amplifier (ADInstruments PowerLab) registered the EGG signal (Figures 1–3).

As we were interested in assessing the coupling between bodily self-consciousness and the physiology of each main segment of the gastrointestinal tract, we waited until the pill went through the pylorus (as marked by a $\geq$2 pH units sudden increase: see above) to repeat the virtual reality experience. This normally occurred within 2–5 h from the ingestion of the capsule. At that point, we administered again the embreathment illusion, this time recording only small bowel data from the SmartPill. When the capsule entered the large bowel (as marked by a $\geq$1 pH unit decrease lasting for at least 10 min, typically observed after 2–6 h from the stomach-small bowel transition: cf. above), we administered the illusion again for the third and last time, always logging SmartPill data for each experimental condition (Figure 1).

After the first 6 h from the beginning of the experiment, participants were provided with a meal. After the first 8 h, they could smoke again. After 3 days, they were allowed to drink alcohol as usual. During the pauses between the stomach and small bowel data collection and between the small and large bowel, they underwent subjective and objective tests of interoception (see Materials section *Measures of interoception* and the supplemental information) and then were free to work or study as they pleased, although they had to avoid strenuous physical exercise. Finally, after the last experimental condition of the large bowel was over, participants could leave the lab. However, they kept the receiver with them, so that they could check the gut physiological parameters for themselves until the capsule stopped transmitting data and was expelled through defecation, ordinarily 10–73 h after ingestion (Lee et al., 2014).

QUANTIFICATION AND STATISTICAL ANALYSIS

SmartPill data pre-processing

Raw SmartPill data were downloaded from the receiver and exported as.txt files. A custom MATLAB algorithm converted relative timestamps in absolute times, so that each event (e.g. beginning and end of each experimental condition) was paired to a definite hh:mm:ss:ms string. Then, the algorithm calculated the mean pH, pressure, and temperature values recorded in each experimental condition as the average of all data points between the beginning and the end of each condition. We also computed the gastric, small bowel, large bowel, and whole gut transit times of the capsule (Lee et al., 2014) to check whether any subject displayed anomalies in their gastric physiology. 30 out of 31 subjects had normal transit times, while the remaining subject had an abnormal large bowel transit time ($\gg$ 59 h, cf. Saad, 2016). Consequently, his SmartPill data were discarded.

EGG data pre-processing

Raw EGG recordings were visually inspected to remove artifacts due to body movements. A 0.016–0.15 Hz bandpass filter removed pink noise and unwanted higher frequencies that are ordinarily associated with cardiac, respiratory, and small bowel activity (cf. Koch and Stern, 2003). The artifact-free tracings thus obtained were then used to extract the EGG peak frequency for each subject and experimental condition (Figure 3). EGG spectral density was computed using Welch's method on 200 s time windows with 150 s overlap (Rebollo et al., 2018). EGG peak frequency was defined as the maximum periodogram peak in the 'normogastric' range, i.e. the range of frequencies that is compatible with the number of stomach contractions in healthy individuals (0.033–0.066 Hz $\sim$ 2–4 cycles per minute; cf. Rebollo et al., 2018). The whole

EGG analysis procedure was performed with BrainVision Analyzer (Brain Products GmbH) and the MATLAB FieldTrip toolbox (Oostenveld et al., 2011).

VAS questionnaire data pre-processing

Raw bodily self-consciousness ratings provided by the subjects through the VAS questionnaire in the virtual reality GUI were exported, then matched with the average pH, pressure, temperature, and EGG peak frequency values computed for each participant, each experimental condition, and each gastro-intestinal district (stomach, small bowel, large bowel).

Statistical data analysis

We used R (version 3.6.1) and the R *lme4* package (Bates et al., 2015) to perform a linear mixed-effects analysis of the data. We modeled how much ratings of perceived body ownership, agency, location, disembodiment, and multiple bodies (see above and Table 1) changed depending on the experimental conditions, the gastro-intestinal (GI) region, and, most importantly, the mean pH, pressure, temperature, and peak frequency values recorded in each experimental condition.

We built two distinct mixed-effects models. Model 1 (SmartPill model) tested the influence of pH, pressure, and temperature of the three GI regions (stomach, small bowel, and large bowel) over bodily self-consciousness. The dependent variable was the whole set of bodily self-consciousness VAS ratings. As fixed effects, the model had the experimental *condition*, i.e. human-avatar sensory congruency (two levels: congruent and incongruent), the VAS *item* (five levels: perceived ownership, agency, location, disembodiment, and two bodies: see Table 1), the GI *region* (three levels: stomach, small bowel, large bowel) and the condition-specific *pH* (continuous), *pressure* (continuous), and *temperature* (continuous).

Model 2 (EGG model) assessed the influence of EGG peak frequencies over bodily self-consciousness. Since EGG peak frequencies are a specific measure of stomach activity, here the dependent variable was a subset of bodily self-consciousness VAS ratings, namely, those collected after the first embreathment illusion induction, when the pill was in the stomach. Like Model 1, also Model 2 featured condition, item, and GI region as factors, but replaced pH, pressure, and temperature with condition-specific *EGG peak frequencies* (continuous).

In both models, fixed effects were tested for interactions with each other. Continuous fixed effects were also group-mean-centred, subtracting the mean of stomach pH from stomach pH values, the mean of small bowel pH from small bowel pH values, and so forth. To control for confounding effects due to individual variability, both models included by-subject random intercepts and Model 1 also had by-condition random slopes. Overall, each mixed model was specified as follows.

Model 1 (SmartPill)

VAS ∼ condition * item * GI region * (pH + pressure + temperature) + (condition | subject), data = SmartPill, control = lmerControl(optimizer = "bobyqa").

Model 2 (EGG)

Stomach VAS ∼ condition * item * EGG peak frequency + (1 | subject), data = EGG, control = lmerControl (optimizer = "bobyqa").

To minimise the chance of Type 1 errors (Luke, 2017), models were fitted with Restricted Maximum Likelihood (REML) and p values were obtained through Type II ANOVA with Satterthwaite's method (Satterthwaite, 1941), as implemented in the *lmerTest* package (Kuznetsova et al., 2017). Statistically significant interactions were followed up with post-hoc tests of the simple effects involving gut physiological parameters, experimental conditions, and bodily self-consciousness ratings against the null hypothesis of a slope equal to zero. All post-hoc tests used Kenward-Roger degrees of freedom (Kenward and Roger, 1997) and were performed via the *emmeans* package to obtain estimated marginal means (EMMs). EMMs were then plotted with the *emmip* function. The percentage of variance explained by each mixed-effects model (Johnson, 2014) was computed through the *r.squaredGLMM* function of Kamil Bartoń's MuMIn Package.

Model 1 converged successfully with no errors and no warnings. The model had a marginal $R^2 = 0.40$ and a conditional $R^2 = 0.61$. Visual inspection of the residual plots did not reveal any obvious deviation from homoscedasticity. Residuals were not normally distributed (Shapiro-Wilk normality test, p < 0.05), but linear models are robust against violations of normality (Gelman et al., 2007). As for collinearity, all independent variables and their products had a GVIF^(1/(2*Df)) < 7. The ratio between the number of data points (n = 855) and the number of estimated parameters (k = 120) was n/k = 7.125, above the minimum ratio of n/k = 3 (see Harrison et al., 2018). Thus, the model was not overparametrized.

Model 2 converged successfully with no errors and no convergence warnings. The model had a marginal $R^2 = 0.37$ and a conditional $R^2 = 0.57$. Visual inspection of the residual plots did not reveal any obvious deviation from homoscedasticity. Residuals were not normally distributed (Shapiro-Wilk normality test, p < 0.05), but linear models are robust against violations of normality (Gelman et al., 2007). As for collinearity, all independent variables and their products had a GVIF^(1/(2*Df)) < 3. The ratio between the number of data points (n = 260) and the number of estimated parameters (k = 20) was n/k = 13, above the minimum ratio of n/k = 3 (see Harrison et al., 2018). Thus, the model was not overparametrized.